

Sintering Behavior of Porous Wall Tile Bodies During Fast Single-Firing Process

Sidnei José Gomes Sousa, José Nilson França de Holanda*

Laboratory of Advanced Materials, State University of Northern Fluminense,
28013-602 Campos dos Goytacazes - RJ, Brazil

Received: November 23, 2003; Revised: March 13, 2005

In ceramic wall tile processing, fast single-firing cycles have been widely used. In this investigation a fast single-firing porous wall tile mixture was prepared using raw materials from the North Fluminense region. Specimens were obtained by uniaxial pressing and sintered in air at various temperatures (1080 – 1200 °C) using a fast-firing cycle (60 minutes). Evolution of the microstructure was followed by XRD and SEM. The results revealed that the main phases formed during the sintering step are anorthite, gehlenite and hematite. It appears that the sintering process is characterized by the presence of a small amount of a liquid phase below 1140 °C. As a result, the microstructure of the ceramic bodies showed a network of small dense zones interconnected with a porous phase. In addition, the strength of the material below 1140 °C appeared to be related to the type and quantity of crystalline phases in the sintered bodies.

Keywords: wall tile, sintering, properties, microstructure

1. Introduction

In the ceramic industry, single-firing is a procedure in which the unfired glaze ware is subject to only one heating cycle to directly obtain the finished product¹. Single-fired wall tiles are formed by dry pressing with moisture content of 4-8%, and the open porosity of the fired ware is usually above 10%. In addition, the flexural strength of the wall tiles should be higher than 15 MPa (for thickness < 7.5 mm) and 12 MPa (for thickness > 7.5 mm), according to Brazilian standard NBR 13818². They are therefore to be included in Group BIII. In the manufacture of this kind of product, the main raw materials are kaolinitic and illitic clays, and with varying carbonate and quartz contents³⁻⁴.

It is well known that traditional raw materials such as clays have a complex mineralogical composition, which makes the study of sintering behavior rather difficult. During sintering of phyllosilicates and associated minerals like quartz, feldspar, calcite, dolomite and hematite, a series of phase transformations occur which determine the final properties of the ceramic products⁵. In the area of mineral raw materials, we must first consider the clay minerals, mainly kaolinite. This clay mineral is often used due to its suitable properties and because it is part of the mineralogical composition of many clay-based ceramics⁶.

In south-eastern Brazil (Campos-RJ), there are important sedimentary clayey mineral deposits, which hold kaolinitic clays⁷. These clays have been extensively characterized for applications in the red ceramic industry⁸. However, for their use in the ceramic tiles industry, only limited studies have been carried out. Presently, the local ceramic industry produces mainly red ceramic products such as dense bricks, ceramic blocks and roofing tiles. The development of products with a higher aggregate value, such as porous wall tile, using clayey materials from Campos-RJ is very important for the economic development of the region.

The main aim of this work is to study the sintering behavior of porous wall tile bodies during fast single-firing using raw materials from the Campos-RJ region. The following techniques were used: X-ray diffraction (XRD), thermogravimetry (TG/DTG), differential thermal analysis (DTA), and scanning electron microscopy (SEM). In addition, correlations between the microstructure of the sintered bodies and their physical-mechanical properties have been made.

2. Materials and Methods

The ceramic paste was formed from a mixture of red kaolinitic clay from Campos-RJ, a calcareous from Italva-RJ and commercial quartz. The composition of the mix used was as follows: red clay 70 wt. (%), calcareous 15 wt. (%) and quartz 15 wt. (%)⁹.

The raw materials were dry ground using a laboratory mill, with 4% screening residue and the mix passed through a 250 mesh (63 µm) screen. The dry-ground powders were granulated in a laboratory granulator with moisture content of 14% (moisture mass/dry mass). After adjusting the moisture content to 7%, the granules were held in a dessicator for 24 hours to homogenize its moisture content. The granule-size distribution of the granulated powder was determined by sieving, according to NBR-7181-84.

X-ray diffraction analysis was done with a Seifert URD-65 diffractometer, using monochromatic Cu-K_α radiation. The phases were identified from the peak position and intensities, using reference data from the JCPDS handbook¹⁰.

Simultaneous DTA/TGA/DTG measurements were carried out in a TA Instruments SDT-2960. The measurements were carried out in air atmosphere from room temperature up to 1150 °C at a heating rate of 10 °C.min⁻¹.

Rectangular ceramic bodies (115 x 25 x 6.75 mm³) were obtained by uniaxial pressing at 35 MPa to render apparent densities of 1.9 g.cm⁻³, upon drying. After pressing, the green ceramic bodies were dried for 24 hours at 110 °C and sintered in a fast-firing laboratory kiln in the 1080-1200 °C maximum temperature range with a fast-firing cycle (~ 60 min). The maximum temperatures correspond to temperatures used during firing of industrial ceramic tiles. The measurements carried out on the sintered ceramic bodies included: linear shrinkage, water absorption and apparent density. In addition, the flexural strength was determined with a three-point bending test (model 1125 Instron) at a loading rate of 0.5 mm.min⁻¹.

A Zeiss DSM 962 scanning electron microscope was used to examine the microstructure of the sintered samples. The phases present in the sintered bodies were identified by X-ray diffraction analysis.

3. Results and Discussion

Figure 1 shows the granule size distribution of the granulated

*e-mail: holanda@uenf.br

powder. It can be observed that the paste falls in the 150-250 μm granule-size range. The purpose of granulation was to improve compaction of the ceramic paste.

Figure 2 shows the X-ray diffractogram of the ceramic paste. The sample is mainly constituted of clay minerals, quartz (SiO_2), calcite (CaCO_3) and gibbsite ($\text{Al}_2(\text{OH})_6$). The clay minerals are a mixture of kaolinite ($\text{Al}_2\text{O}_3 \cdot 2\text{SiO}_2 \cdot 2\text{H}_2\text{O}$) and illite/mica ($\text{K}_x(\text{Al,Mg})_4(\text{Si,Al})_8\text{O}_{20}(\text{OH})_4 \cdot n\text{H}_2\text{O}$, with $x < 1$), but the main clay mineral is kaolinite. In addition, traces of potassium feldspar (KAlSi_3O_8), dolomite ($\text{CaMg}(\text{CO}_3)_2$) and goethite ($\alpha\text{-Fe}_2\text{O}_3 \cdot \text{H}_2\text{O}$) were also identified.

The X-ray diffractograms of the ceramic bodies sintered at temperatures in the range 1080-1160 $^\circ\text{C}$ are shown in Figure 3. The increase in sintering temperature for single firing ceramic pastes exceeds the energy threshold of the reactivity of the materials, and produces a series of reactions and transformations that lead to the formation of new phases and the disappearance of others¹¹. The phases present at 1080 $^\circ\text{C}$ were quartz (SiO_2), hematite (Fe_2O_3), anorthite ($\text{CaO} \cdot \text{Al}_2\text{O}_3 \cdot 2\text{SiO}_2$), gehlenite ($2\text{CaO} \cdot \text{Al}_2\text{O}_3 \cdot \text{SiO}_2$) and primary mullite. It can be observed that the kaolinite, gibbsite, calcite, dolomite and goethite peaks disappeared and the quartz peaks remained. As the temperature increased, anorthite and hematite peak intensities began to increase and the quartz peak intensities began to decrease.

Figure 4 shows the DTA/TGA/DTG curves of the ceramic paste. It can be seen that the paste exhibits four characteristic endothermic valleys at 42, 255, 489 and 710 $^\circ\text{C}$. The first endothermic valley (mass loss 1.101%) is due to removal of physically adsorbed water, typical of kaolinitic materials. The second endothermic valley (mass loss 1.952%) is due to removal of hydroxides crystallization water. The third endothermic valley (mass loss 5.757%) is due to dehydroxylation of the silicate lattice, leading to the formation of metakaolinite ($\text{Al}_2\text{O}_3 \cdot 2\text{SiO}_2$). The fourth endothermic valley (mass loss 5.962%) is due to thermal decomposition of calcite to form calcium oxide (CaO) and CO_2 . The small exothermic peak at 950 $^\circ\text{C}$ is due to further disruption of the lattice, and is probably related to the formation of new crystalline phases such as Si containing $\gamma\text{-Al}_2\text{O}_3$ with a spinel structure and/or 2:1 mullite¹¹⁻¹². The phase changes with sintering temperature, in Figure 3, suggest the following reactions. First gehlenite appears from the metakaolinite and calcium oxide reaction. Later, anorthite is formed from the gehlenite and metakaolinite reaction⁶⁻¹³. The DTA curve reveals only one exothermic phenomenon at 950 $^\circ\text{C}$, and is characterized by a smoother peak. It seems that the series of reactions, associated with the metakaolinite structural reorganization, could take place simultaneously and progressively.

The fractured surfaces of the specimens sintered at 1080 and 1200 $^\circ\text{C}$ are shown in Figure 5. At 1080 $^\circ\text{C}$ (Figure 5a) the microstructure reveals regions that contain large pores, resulting from carbonate decomposition. These regions are connected with dense zones. At 1200 $^\circ\text{C}$ the open porosity decreases. Some glassy phase also begins to emerge.

The gresification diagram of the sintered bodies is shown in Figure 6. It can be seen that the variation of linear shrinkage and water absorption (open porosity) is lower in a wider firing range (1080-1140 $^\circ\text{C}$), characterized by lower linear shrinkage values (1.96-2.06%) and higher open porosity values (19.54-19.59%). This behavior is due to the calcium oxide formed during carbonate decomposition, as seen in Figure 4. During pre-heating in the temperature range 800-900 $^\circ\text{C}$, a reaction between the amorphous phase, produced by the decomposition of kaolinite, and calcium oxide occurs with formation of crystalline phases such as anorthite and gehlenite that affect liquid phase formation¹⁴. This reaction sequence and the reduced liquid phase formation improve the ceramic bodies with increased porosity and a wider firing range. Above 1140 $^\circ\text{C}$ some changes occurred. It can be noted from Figure 6 that the linear

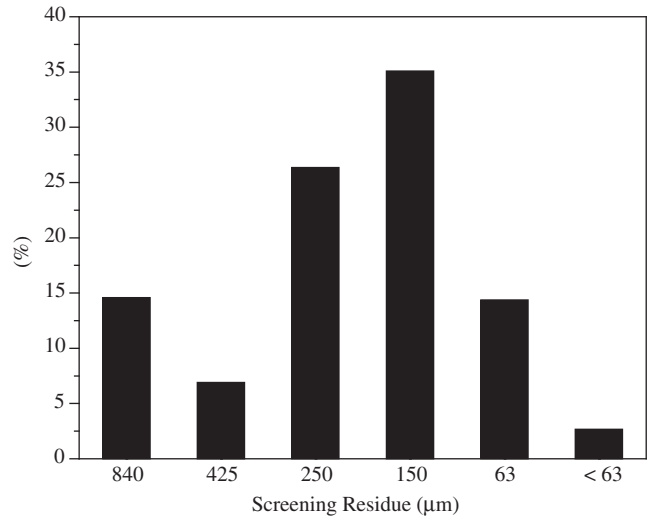


Figure 1. Granulated powder size distribution by sieving.

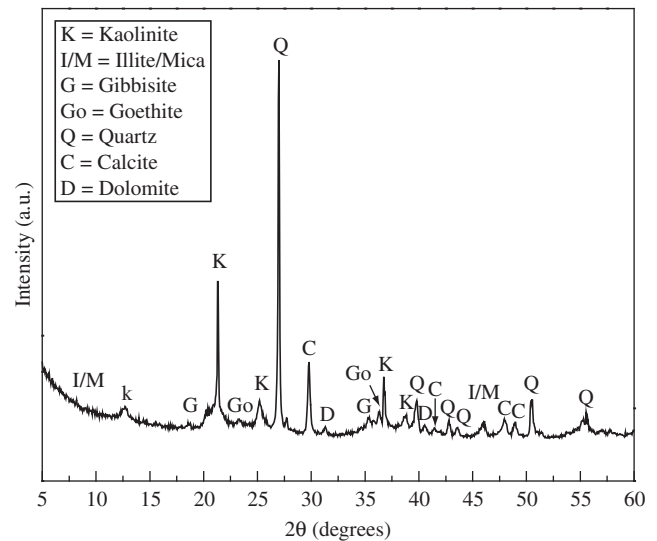


Figure 2. X-ray diffraction pattern of the ceramic paste.

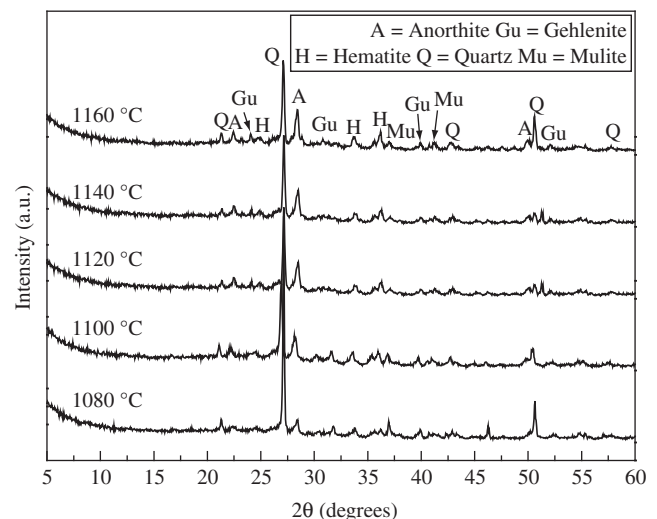


Figure 3. X-ray diffraction patterns of the ceramic paste after sintering at various temperatures.

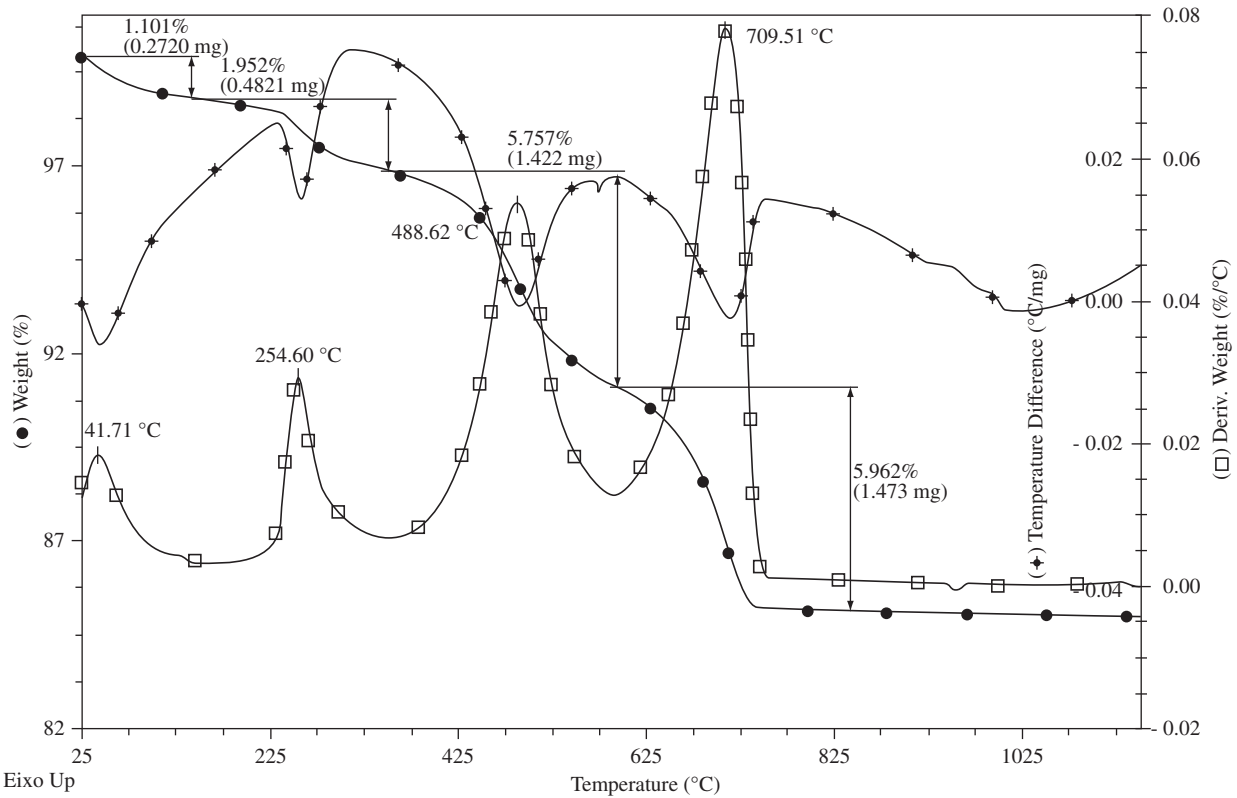
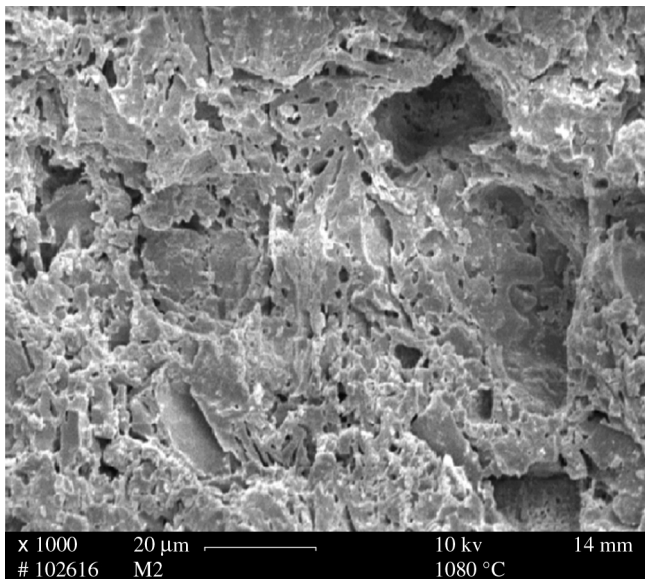
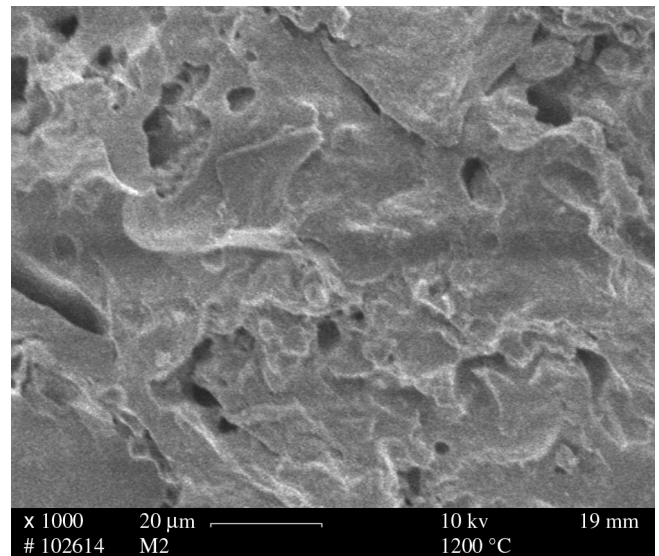


Figure 4. DTA/TG/DTG curves of the ceramic paste.



(a)



(b)

Figure 5. Fractured surface of the ceramic bodies sintered: a) 1080 °C; b) 1200 °C.

shrinkage values vary considerably (2.06-3.74%). Water absorption also varies significantly (16.91-19.65%).

Figure 7 shows apparent density as a function of sintering temperature. It can be seen that the apparent density of the ceramic bodies is almost constant in the range 1080-1140 °C, with only a small variation (1.76-1.78 g.cm⁻³). Above 1140 °C, the range is higher (1.79-1.84 g.cm⁻³). This behavior is related to increase in the glassy phase and consequent predominance (probably) of the viscous flow sintering mechanism for material densification. Moreover, crystalliza-

tion of ceramic phases such as gehlenite and anorthite from metakaolinite contributes to higher densification in this temperature range.

Figure 8 shows the flexural strength of the ceramic bodies as a function of sintering temperature. As can be observed, the values of flexural strength increase with sintering temperature (11.73-17.34 MPa). In the range 1080-1140 °C, the strength of the ceramic bodies appears to be related to the type and quantity of crystalline phases rather than porosity. Above 1140 °C, the values of flexural strength (19.19-23.77 MPa) increase with densification. In

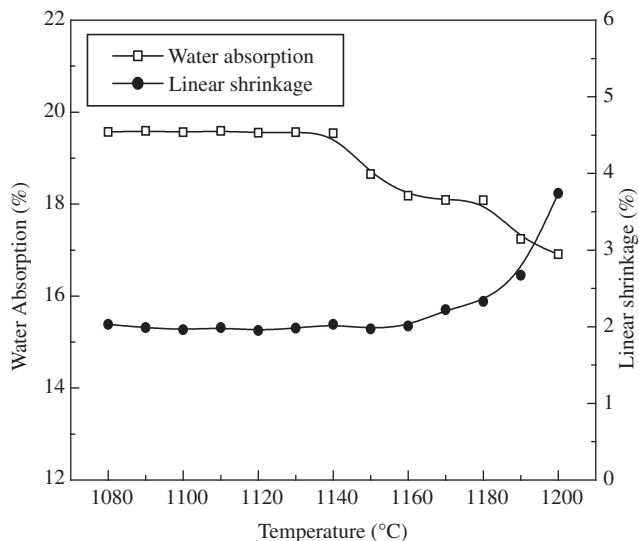


Figure 6. Gresification curve of the ceramic paste.

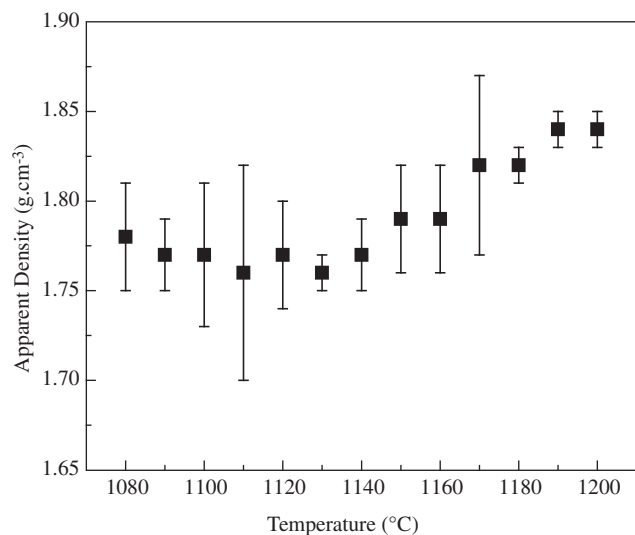


Figure 7. Apparent density as a function of sintering temperature.

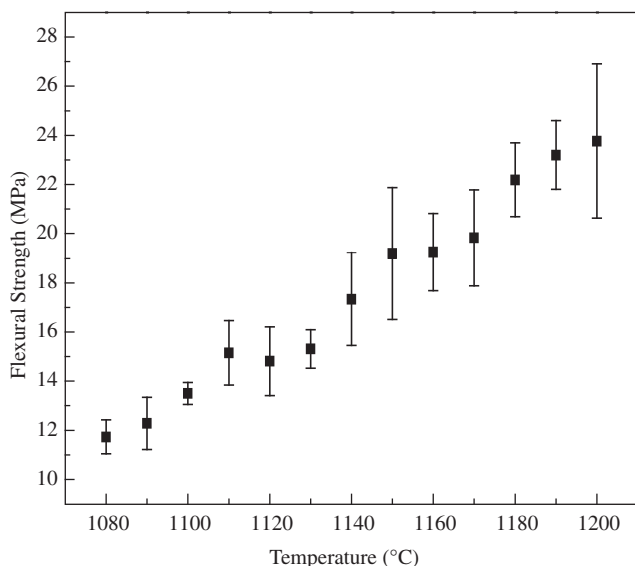


Figure 8. Flexural strength as a function of sintering temperature.

addition, a correlation between flexural strength and water absorption (open porosity) can be observed.

4. Conclusions

The ceramic paste presented high dimensional stability (low linear shrinkage) between 1080-1140 °C. In addition, variation of water absorption is not relevant in this temperature range, and apparent density is almost constant. Above 1140 °C variations in the different properties occurred, due to formation of the liquid phase.

Two sintering ranges were observed. In the first range (1080-1140 °C), sintering is characterized by a small amount of the liquid phase. Above 1140 °C significant changes occurred, probably due to predominance of viscous flux sintering mechanism for densification of the ceramic bodies.

The results revealed that the main phases formed during the sintering step are gehlenite, anorthite and hematite. In general, the microstructure of the ceramic bodies showed a network of small dense zones interconnected by a porous phase.

Acknowledgments

This work was partially financed by CAPES, FAPERJ and CNPq, whose support is gratefully acknowledged.

References

- Escardino A. Single-fired ceramic wall tile manufacture. *Tile & Brick Int.* 1993; 9(1):14-19.
- NBR 13818. *Ensaios para Quantificação das Características Físico-químicas das Placas Cerâmicas*. Rio de Janeiro (Brasil): Associação Brasileira de Normas Técnicas; 1997.
- Barba A, Felú C, García J, Ginés F, Sánchez E, Sanz V, et al. *Materias Primas Para la Fabricación de Soportes de Baldosas Cerámicas*. 1a ed. Castellón: Instituto de Tecnología Cerámica; 1997.
- Zauberas RT, Riella HG. Defeitos de queima causados pelo quartzo em monoporosas. *Cerâm Ind.* 2001; 6(2):40-45.
- Jordán MM, Sanfeliu T, De La Fuente C. Firing transformations of tertiary clays used in the manufacturing of Ceramic tile bodies. *Appl Clay Sci.* 2001; 20(1-2):87-95.
- Traoré K, Kabré TS, Blanchart P. Gehlenite and anorthite crystallization from kaolinite and calcite mix. *Ceram Int.* 2003; 29(4):377-383.
- Souza GP, Sanchez R, Holanda JNF. Characteristics and physical-mechanical properties of fired kaolinitic materials. *Cerâmica.* 2002; 48(306):102-107.
- Souza GP, Sanchez R, Holanda JNF. Thermal and structural characterization of brazilian southeastern kaolinitic clays. *J Therm Anal Cal.* 2003; 73(1):293-305.
- Sousa SJG. *Formulação e Caracterização de Massas Cerâmicas Para Revestimento Poroso de Base Vermelha Utilizando Matérias-Primas da Região de Campos dos Goytacazes-RJ*. [Dissertação de Mestrado]. Campos dos Goytacazes (RJ): Universidade Estadual do Norte Fluminense; 2003.
- JCPDS – *Powder Diffraction File*. Ed. International Center for Diffraction Data. Philadelphia, USA. 1995.
- Chen CY, Lan GS, Tuan WH. Microstructural evolution of mullite during the sintering of kaolin powder compacts. *Ceram Int.* 2000; 26:715-20.
- McConville CJ, Lee WE, Sharp JH. Microstructural evolution in fired kaolinite. *Brit Ceram Transac.* 1998; 97(4):162-168.
- El-Didamony H, Assal HH, Hassan HS, Abd El-Ghfour NG. The thermal behavior of clay and calcareous clays containing different lime contents. *Ind Ceram.* 1998; 18(2):91-98.
- Cava S, Paskocimas CA, Longo E. Influência do teor de CaO no comportamento de formulações de revestimentos cerâmicos produzidos por via seca. *Anais do 45º Congresso Brasileiro de Cerâmica*; Mai-Jun 2001 Florianópolis (SC), Brasil. p. 265-278.